FDTD Analysis of EM Wave Propagation in a Space-time-modulated Lossy Transmission Line

Anand Kumar[(1)], and Debdeep Sarkar[(1)]
(1) Dept. of ECE, Indian Institute of Science, Bengaluru, KA 560012, India

Abstract

This paper explores electromagnetic (EM) wave propagation in lossy transmission lines (TLs) with space-time-varying parameters, such as capacitance and inductance, using the Finite-Difference Time-Domain (FDTD) method. It examines the effects of spatial, temporal, and spatio-temporal modulation on wave phenomena, including frequency translation, energy dissipation, and non-reciprocal behavior, while accounting for resistive and dielectric losses. A novel perfectly matched layer (PML) formulation, derived from Telegrapher's equations for lossy, space-time-modulated TLs, is proposed to suppress boundary reflections. The results offer key insights into EM behavior in dynamic lossy systems, paving the way for advanced space-time-modulated devices with applications in frequency mixers, isolators, and energy harvesting.

1 Introduction

Electromagnetic (EM) wave propagation in media with time- and space-varying properties is a transformative area of research in metamaterials and microwave engineering. Space-time-varying systems, where parameters like permittivity, permeability, and conductivity vary across space and time, enable functionalities such as non-reciprocal signal propagation, frequency translation, and EM cloaking [1, 2, 3, 4]. These properties drive innovations in communication systems, radar technologies, and energy-harvesting devices [5, 6, 7].

Transmission lines (TL) with time-varying parameters provide an essential platform for studying space-time-modulated systems [3, 8]. When losses are included, these systems exhibit complex interactions between wave propagation and energy dissipation, creating challenges for accurate modelling. While previous studies have investigated idealized lossless TL or static material properties, the impact of losses on wave behaviour in time-varying media remains an under-explored area [3, 8, 9]. Understanding such effects is crucial for practical applications where real-world systems often include resistive and dielectric losses.

The Finite-Difference Time-Domain (FDTD) method offers a powerful tool for analyzing space-time-modulated systems by solving Maxwell's equations in the time domain [10, 11]. This paper employs FDTD to study EM wave behaviour in lossy TL with space-time-varying constitutive parameters, examining the effects of losses and modulation parameters on wave propagation, frequency translation, and non-reciprocity.

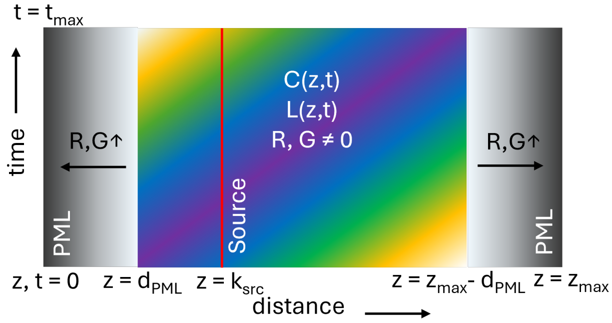

Figure 1. Schematic representation of the lossy TL with space-time-varying capacitance $C(z,t)$ and inductance $L(z,t)$, and non-zero resistance R and conductance G, a wave source, and PML boundaries with exponentially increasing R and G to suppress reflections.

This study aims to:

- Develop an FDTD-based computational framework to model space-time-varying lossy TL.
- Investigate the influence of losses on the propagation characteristics of EM waves, including energy dissipation and wave distortion.
- Explore potential applications of space-time-varying lossy TL in non-reciprocal devices.

The remainder of this paper is structured as follows. Section 2 provides an overview of the FDTD formulation for space-time-varying lossy TL. Section 3 presents the results and insights from the simulations of the FDTD algorithm, including the incorporation of losses, space-time modulation and parametric studies. Finally, Section 4 concludes the paper and discusses future research directions.

2 FDTD Update Equations for Space-time-varying Lossy Transmission Lines

The Telegrapher's equations in a space-time-modulated TL are given by:

$$\frac{\partial C(z,t)v(z,t)}{\partial t} + Gv(z,t) = -\frac{\partial i(z,t)}{\partial z}, \tag{1a}$$

$$\frac{\partial L(z,t)i(z,t)}{\partial t} + Ri(z,t) = -\frac{\partial v(z,t)}{\partial z}. \tag{1b}$$

$C(z,t)$ and $L(z,t)$ are space-time dependent the capacitance and inductance per unit length of the TL, and R and G are the resistance and conductance of the TL due to finite conductivity and the dielectric loss.

Taking finite differences in space and time, (1a) and (1b) yeild (2a) and (2b), respectively.

$$v_k^{n+1} = \left(\frac{\rho_{C-}}{\rho_{C+}}\right) v_k^n - \frac{1}{\rho_{C+}\Delta z}\left[i_{k+0.5}^{n+0.5} - i_{k-0.5}^{n+0.5}\right], \tag{2a}$$

$$i_{k+0.5}^{n+0.5} = \frac{\rho_{L-}}{\rho_{L+}} i_{k+0.5}^{n-0.5} - \frac{1}{\rho_{L+}\Delta z}\left[v_{k+1}^n - v_k^n\right], \tag{2b}$$

Here, $\rho_{C-} = \left(\frac{C_k^n}{\Delta t} - \frac{G}{2}\right)$, $\rho_{C+} = \left(\frac{C_k^{n+1}}{\Delta t} + \frac{G}{2}\right)$, $\rho_{L-} = \left(\frac{L_k^n}{\Delta t} - \frac{R}{2}\right)$ and $\rho_{L+} = \left(\frac{L_k^{n+1}}{\Delta t} + \frac{R}{2}\right)$ with Δz and Δt as the space and time steps.

The incident waveform (V_{inc}) is introduced into the TL using a "one-way" injector at position $k = k_{src}$:

$$\begin{aligned} i_{k_{src}+0.5}^{n+0.5} = {} & \frac{\rho_{L-}}{\rho_{L+}} i_{k_{src}+0.5}^{n-0.5} - \frac{1}{\rho_{L+}\Delta z}\left[v_{k_{src}+1}^n - v_{k_{src}}^n\right] \\ & + \frac{1}{\sqrt{\rho_{L+}}\sqrt{\rho_{C+}}\Delta z} v_{inc,k_{src}}^n \end{aligned} \tag{3}$$

$$\begin{aligned} v_{k_{src}}^{n+1} = {} & \left(\frac{\rho_{C-}}{\rho_{C+}}\right) v_{k_{src}}^n - \frac{1}{\rho_{C+}\Delta z}\left[i_{k_{src}+0.5}^{n+0.5} - i_{k_{src}-0.5}^{n+0.5}\right] \\ & + \frac{1}{\sqrt{\rho_{L+}}\sqrt{\rho_{C+}}\Delta z} v_{inc,k_{src}+0.5}^{n+0.5} \end{aligned} \tag{4}$$

This launches the voltage excitation within the line in only the +z direction.

The TL boundaries at $k' = 0$ and z_{dim} are truncated using a perfectly matched layer (PML) of width d_{PML}. A modified PML for the FDTD method, based on the Telegrapher's equations, is designed by maintaining impedance matching while exponentially increasing losses (R and G) in a distortionless TL, where $\frac{R}{L} = \frac{G}{C}$. The resulting complex propagation constant is given by

$$\gamma = R\sqrt{\frac{C}{L}} + j\omega\sqrt{LC} = \alpha + j\beta. \tag{5}$$

By exponentially increasing the attenuation α within the PML region—from $z = d_{PML}$ toward $z = 0$ and from $z = z_{max} - d_{PML}$ to $z = z_{max}$—wave reflections at the boundaries are effectively suppressed.

3 Results and Analysis

Figure 1 presents a schematic representation of a lossy TL with space-time-varying parameters. The central region incorporates spatio-temporally varying capacitance $C(z,t)$ and inductance $L(z,t)$, alongside nonzero resistance R and conductance G to model the lossy medium. An incident EM wave is injected into the system, with PMLs at the boundaries to mitigate reflections. The resistance and conductance within the PMLs increase exponentially to ensure effective absorption of outgoing waves.

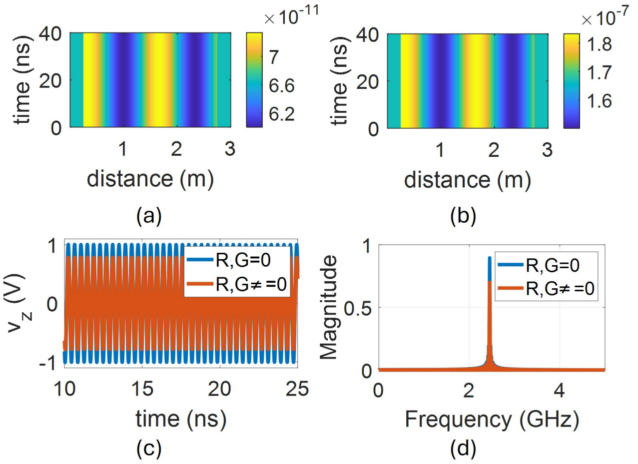

Figure 2. EM wave propagation in a spatially varying TL: (a)-(b) spatiotemporal distributions of $C(z,t)$ and $L(z,t)$, (c) voltage at a fixed position, and (d) frequency spectrum.

3.1 Sinusoidal Spatio-Temporal Variation

For this analysis, the lossy parameters are set as $R = 5\times 10^3 \Omega/m$ and $G = 0.004$ S/m. The characteristic inductance and capacitance are given by $L_0 = \frac{Z_0}{c}$ and $C_0 = \frac{1}{Z_0 c}$, where $Z_0 = 50\ \Omega$ is the characteristic impedance, and c is the speed of light in free space. The TL has a total width of 2.5 m, while the PML region spans $d_{PML} = 80\Delta z$.

The variations in inductance and capacitance follow a sinusoidal profile, defined as:

$$C(z,t) = C_0(1 + \varsigma\sin(\beta_s z - \omega_t t)), \tag{6a}$$

$$L(z,t) = L_0(1 + \varsigma\sin(\beta_s z - \omega_t t)), \tag{6b}$$

where $\beta_s = \frac{2\pi f_s}{c}$ and $\omega_t = 2\pi f_t$, with f_s and f_t denoting the spatial and temporal modulation frequencies, respectively. The modulation index, ς, determines the strength of the variation.

3.1.1 Spatial Variation ($f_s \neq 0, f_t = 0$)

Figure 2 presents the response of an EM wave of frequency $f_0 = 2.45$ GHz propagating through a spatially modulated TL for both lossless ($R,G = 0$) and lossy ($R,G \neq 0$) cases, with $\varsigma = 0.02$. Figures 2(a) and 2(b) illustrate the spatiotemporal variations of $C(z,t)$ and $L(z,t)$ for a spatial modulation frequency of $f_s = 225$ MHz. The temporal voltage response at a fixed position is shown in Fig. 2(c), highlighting a reduction in amplitude due to losses. The corresponding frequency spectrum in Fig. 2(d) indicates attenuation of the fundamental frequency component (f_0) and an overall reduction in spectral magnitude due to dissipation.

3.1.2 Temporal Variation ($f_s = 0, f_t \neq 0$)

Figure 3 illustrates the response of an EM wave in a time-varying TL under both lossless and lossy conditions, with $\varsigma = 0.1$ and $f_0 = 2.45$ GHz. Figures 3(a) and 3(b) depict

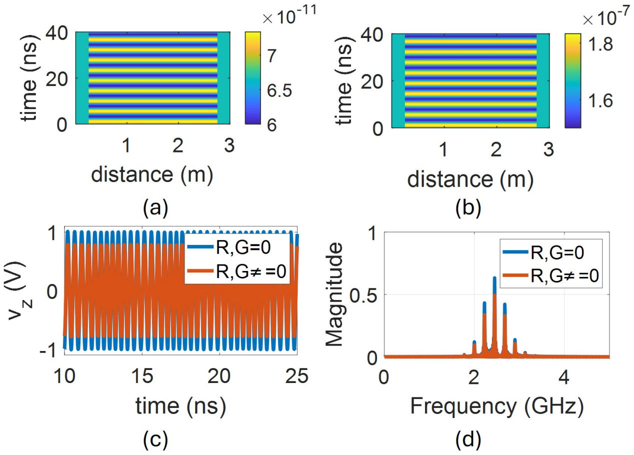

Figure 3. EM wave propagation in a time-varying TL: (a)-(b) spatiotemporal distributions of $C(z,t)$ and $L(z,t)$, (c) modulated voltage signal, and (d) frequency spectrum.

the spatiotemporal variations of $C(z,t)$ and $L(z,t)$ for a temporal modulation frequency of $f_t = 225$ MHz. The modulated voltage waveform, shown in Fig. 3(c), exhibits a reduction in amplitude due to loss. The frequency spectrum in Fig. 3(d) reveals power redistribution among harmonics at $f_0 \pm f_t$, along with an overall reduction in spectral energy.

3.1.3 Spatio-Temporal Variation ($f_s, f_t \neq 0$)

Figure 4 examines EM wave propagation in a space-time-modulated TL, considering a modulation index of $\varsigma = 0.02$ and a wave frequency of $f_0 = 2.45$ GHz. The capacitance and inductance distributions, displayed in Figs. 4(a) and 4(b), correspond to a modulation frequency of $f_t = f_s = f_m = 225$ MHz. The temporal voltage signals for forward and backward propagation are presented in Figs. 4(c) and 4(d), respectively, showing significant attenuation in the lossy case. The associated frequency spectra in Figs. 4(e) and 4(f) highlight energy redistribution into harmonics at $f_0 \pm n f_m$, with greater attenuation observed for the backward-propagating wave. This demonstrates nonreciprocal propagation, where the forward wave retains higher energy compared to the backward wave.

3.2 Parametric Study

This section explores the influence of modulation frequency and modulation index on nonreciprocal wave behavior in lossy space-time-modulated TLs.

3.2.1 Effect of Modulation Frequency

As shown in Fig. 5(a), the modulation frequency f_m plays a critical role in determining spectral energy distribution. For low f_m, energy is significantly redistributed among multiple harmonics, causing greater attenuation at $f_0 = 2.45$ GHz. As f_m increases (up to approximately 200 MHz), the forward-propagating wave stabilizes at a higher amplitude. Conversely, the backward wave undergoes rapid attenuation with increasing f_m, after which it remains highly suppressed, emphasizing the importance of selecting an optimal modulation frequency for maximizing nonreciprocity.

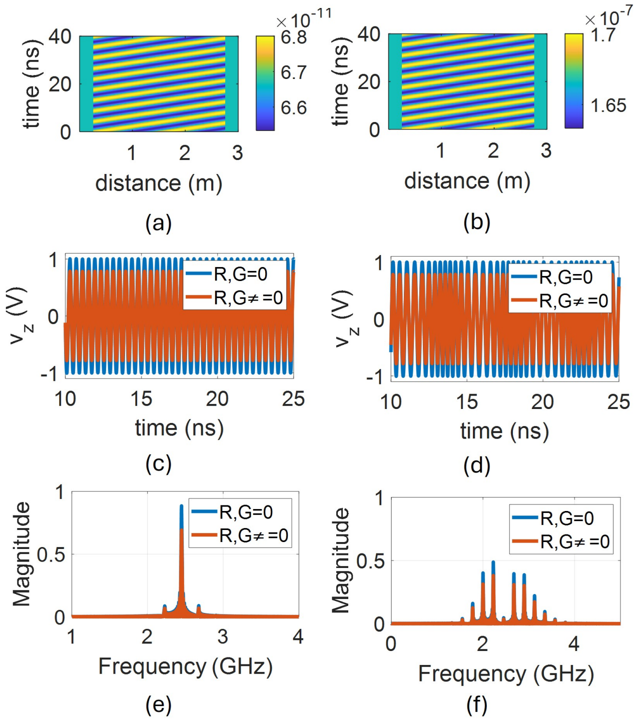

Figure 4. EM wave propagation in a space-time-varying TL: (a)-(b) spatiotemporal distributions of $C(z,t)$ and $L(z,t)$, (c)-(d) voltage signals for forward/backward propagation, and (e)-(f) corresponding frequency spectra.

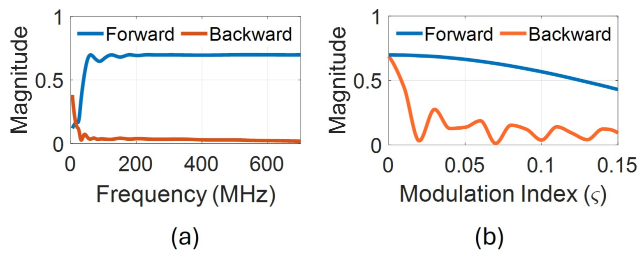

Figure 5. Effect of (a) modulation frequency f_m and (b) modulation index ς on forward and backward propagating EM waves in lossy space-time-modulated TL.

3.2.2 Effect of Modulation Index

The modulation index ς influences wave attenuation and spectral distribution. As illustrated in Fig. 5(b), an increase in ς enhances nonreciprocity by further attenuating the backward wave. However, beyond a certain threshold, stronger modulation induces the generation of additional harmonics, leading to energy dissipation from the fundamental frequency component. This results in a reduction of nonreciprocity, indicating that an optimal ς is necessary to balance energy retention and harmonic suppression.

3.2.3 Effect of R and G

Figure 6 shows the impact of R and G on forward and backward propagating waves in a lossy space-time-modulated

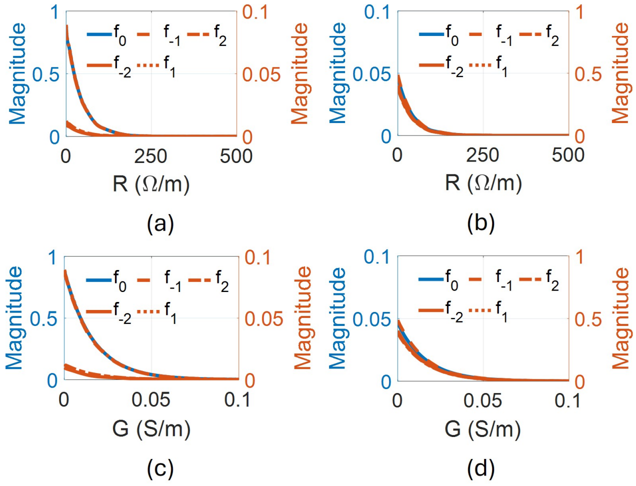

Figure 6. Effect of R on ((a) forward and (b) backward) and G on ((c) forward and (d) backward) propagating EM waves in lossy space-time modulated TL.

TL, focusing on the fundamental frequency f_0 and its harmonics ($f_{\pm 1}$, $f_{\pm 2}$). Figures 6(a) and 6(b) illustrate that as R increases, all frequency components experience significant attenuation, with f_0 showing the most decay. Similarly, Figs. 6(c) and 6(d) demonstrate that increasing G causes comparable attenuation. Both parameters strongly affect energy distribution and nonreciprocal behavior, with higher R and G values leading to greater power loss, reduced wave amplitudes, and limited nonreciprocity.

4 Conclusion

This paper investigates EM wave propagation in lossy transmission lines with space-time-varying parameters using the Finite-Difference Time-Domain (FDTD) method. It examines the impact of spatial, temporal, and spatio-temporal modulation on wave characteristics such as frequency translation, non-reciprocity, and energy dissipation, while addressing resistive and dielectric losses. A novel perfectly matched layer (PML) is introduced for accurate boundary handling and minimized reflections. The study explores the influence of modulation frequency, modulation index, and loss effects on non-reciprocal wave behavior. These findings provide guidelines for optimizing space-time-modulated transmission lines and offer insights into designing advanced devices like isolators, frequency mixers, and energy harvesters, with potential for further exploration of non-linear effects and experimental validation.

5 Acknowledgements

The authors thank the Indian Space Research Organisation (ISRO) (Grant No. ISTC/EEC/DS/492) and the Prime Minister's Research Fellowship (Grant No. TF/PMRF-22-3965), Ministry of Education, Govt. of India, for support.

References

[1] C. Caloz and T. Itoh, *Electromagnetic Metamaterials: Transmission Line Theory and Microwave Applications*. John Wiley & Sons, 2005.

[2] C. Caloz, Z. -L. Deck-Léger, A. Bahrami, O. C. Vicente and Z. Li, “Generalized space-time engineered modulation (GSTEM) metamaterials: A global and extended perspective,” *IEEE Antennas and Propagation Magazine*, **65**, 4, 2023, pp. 50-60.

[3] A. Kumar and D. Sarkar, “FDTD Analysis of Space-time Metamaterials using Modulated TVTLs for Frequency Translation, Mixing and Non-reciprocity,” *2023 53rd European Microwave Conference (EuMC)*, Berlin, Germany, 2023, pp. 311-314.

[4] S. Taravati and A. A. Kishk, "Space-Time Modulation: Principles and Applications," in IEEE Microwave Magazine, **21**, 4, 2020, pp. 30-56.

[5] A. Galiffi, P. A. Huidobro, and J. B. Pendry, “Broadband nonreciprocal amplification in luminal metamaterials,” *Physical Review Letters*, **123**, 20, 2019, pp. 206101.

[6] J. B. Pendry, D. Schurig, and D. R. Smith, “Controlling electromagnetic fields,” *Science*, **312**, 5781, 2006, pp. 1780-1782.

[7] A. Kumar, S. Kongari, Y. Chandrakapure, and D. Sarkar, “Multi-functional metasurface as a transmissive/reflective FSS and an on-air frequency mixer,” *Nature Scientific Reports*, **14**, pp. 13874, 2024.

[8] A. Kumar, J. C. Dash and D. Sarkar, “Computational Techniques for Design and Analysis of Time-Varying Capacitor loaded Transmission Lines using FDTD and Simulink,” *IEEE Journal on Multiscale and Multiphysics Computational Techniques*, **7**, 2022, pp. 228-235.

[9] A. Kumar, J. C. Dash and D. Sarkar, “Frequency Translation of EM Waves using Time-Varying Dielectrics: Insights on Slab-Width and Duration of Permittivity Variation using FDTD,” *2021 IEEE Indian Conference on Antennas and Propagation (InCAP)*, 2021, pp. 316-319.

[10] D. Sarkar, *FDTD Analysis of Guided Electromagnetic Wave Interaction with Time Modulated Dielectric Medium*. Springer, 2022.

[11] A. Taflove, S.C. Hagness, and M. Piket-May, “Computational electromagnetics: the finite-difference time-domain method,” *The Electrical Engineering Handbook*, **3**, 629-670, 2005, pp. 15.